MIT Libraries | DSpace@MIT

MIT Open Access Articles

THE CHEMICAL COMPOSITIONS OF VERY METAL-POOR STARS HD 122563 AND HD 140283: A VIEW FROM THE INFRARED

Massachusetts Institute of Technology

THE CHEMICAL COMPOSITIONS OF VERY METAL-POOR STARS HD 122563 AND HD 140283: A VIEW FROM THE INFRARED

Melike Afşar[1,2], Christopher Sneden[2], Anna Frebel[3], Hwihyun Kim[2,4], Gregory N. Mace[2], Kyle F. Kaplan[2],
Hye-In Lee[5], Heeyoung Oh[4], Jae Sok Oh[4], Soojong Pak[5], Chan Park[4], Michael D. Pavel[2,6],
In-Soo Yuk[4], and Daniel T. Jaffe[2]

[1] Department of Astronomy and Space Sciences, Ege University, 35100 Bornova, İzmir, Turkey; melike.afsar@ege.edu.tr
[2] Department of Astronomy and McDonald Observatory, The University of Texas, Austin, TX 78712, USA;
chris@astro.as.utexas.edu, dtj@astro.as.utexas.edu, hwihyun@astro.as.utexas.edu, mace@astro.as.utexas.edu
[3] Kavli Institute for Astrophysics and Space Research and Department of Physics, Massachusetts Institute of Technology, Cambridge, MA 02139, USA;
afrebel@mit.edu
[4] Korea Astronomy and Space Science Institute (KASI), Daejeon, Korea; hyoh@kasi.re.kr, ojs001@kasi.re.kr, chanpark@kasi.re.kr, yukis@kasi.re.kr
[5] School of Space Research (IR Lab), Kyung Hee University 1732 Deokyoungdaero, Giheung-gu, Yongin-si Gyeonggi-do 446-701, Korea;
huynhanh7@khu.ac.kr, soojong@khu.ac.kr
[6] Institute for Astrophysical Research, Boston University, Boston, MA 02215, USA; michaeldpavel@gmail.com
Received 2015 October 25; accepted 2016 January 10; published 2016 March 3

ABSTRACT

From high resolution ($R \simeq 45,000$), high signal-to-noise ratio ($S/N > 400$) spectra gathered with the Immersion Grating Infrared Spectrograph (IGRINS) in the H and K photometric bands, we have derived elemental abundances of two bright, well-known metal-poor halo stars: the red giant HD 122563 and the subgiant HD 140283. Since these stars have metallicities approaching $[Fe/H] = -3$, their absorption features are generally very weak. Neutral-species lines of Mg, Si, S and Ca are detectable, as well as those of the light odd-Z elements Na and Al. The derived IR-based abundances agree with those obtained from optical-wavelength spectra. For Mg and Si the abundances from the infrared transitions are improvements to those derived from shorter wavelength data. Many useful OH and CO lines can be detected in the IGRINS HD 122563 spectrum, from which derived O and C abundances are consistent to those obtained from the traditional [O I] and CH features. IGRINS high resolutions H- and K-band spectroscopy offers promising ways to determine more reliable abundances for additional metal-poor stars whose optical features are either not detectable, or too weak, or are based on lines with analytical difficulties.

Key words: instrumentation: spectrographs – stars: abundances – stars: atmospheres – stars: individual (HD 122563, HD 140283) – stars: Population II

Supporting material: machine-readable tables

1. INTRODUCTION

Element production in the early Galaxy commenced quickly with the explosive deaths of high-mass stars. Their ejecta were gathered up to form the low-mass very metal-poor stars that we observe today. These stars are powerful tracers of the onset of Galactic nucleosynthesis because they live long enough to still be observable today. Their atmospheres preserve information on the chemical history of the very early Milky Way. The spectroscopic task is to derive accurate abundances for as many elements as possible of important nucleosynthetic groups (LiBeCNO, α, light odd-Z, Fe-peak, and neutron-capture) in low metallicity stars to constrain our ideas about early Galactic chemical evolution.

Low-metallicity stars exhibit weak and uncrowded absorption spectra, which makes abundance analyses relatively easy. However, this asset is also a liability, because the number of lines detectable for many elements drops precipitously as metallicities decline from solar to the ultra-metal-poor regime. It is difficult to find any absorption features at all in the record-setting halo stars with[7] $[Fe/H] < -7$, such as SMSS J031300.36–670839.3 (e.g., Figure 1 of Keller et al. 2014). Indeed, in the abundance literature for stars with

$[Fe/H] \lesssim -2.5$, many elements are represented only by their resonance or very low-excitation lines. Species relying on 1–3 lines include for example Na I (the D-lines); Al I (3961 Å); and Mn I (the 4030 Å resonance triplet). This is unfortunate, because abundances derived from very strong low-excitation lines sometimes are very discordant with those derived from weaker high-excitation lines.

High-resolution spectra in different wavelength regimes can provide additional absorption features to improve the reliability of many abundances in metal-poor stars. The vacuum ultraviolet contains ionized species to complement many of the elements that have only neutral-species features in the optical spectral region. But only a small number of low metallicity stars have ever been observed at high spectral resolution in the UV with the *Hubble Space Telescope*. That list of stars is unlikely to grow significantly in the near future.

The infrared wavelength regime contains many neutral-species transitions of the more abundant light and Fe-group elements. High-resolution IR spectra now can be obtained with ground based facilities, such as the Very Large Telescope/CRIRES[8] (Kaeufl et al. 2004), and the Gemini/GNIRS[9] (Elias et al. 2006).

---

[7] We adopt the standard spectroscopic notation (Wallerstein & Helfer 1959) that for elements A and B, $[A/B] \equiv \log_{10}(N_A/N_B)_\star - \log_{10}(N_A/N_B)_\odot$. We use the definition $\log \epsilon(A) \equiv \log_{10}(N_A/N_H) + 12.0$, and equate metallicity with the stellar [Fe/H] value.

[8] CRyogenic high-resolution InfraRed Echelle Spectrograph; http://www.eso.org/sci/facilities/paranal/instruments/crires.html; currently undergoing an upgrade.

[9] Gemini Near Infra-Red Spectrograph; http://www.gemini.edu/sciops/instruments/gnirs.

Table 1
Program Star Parameters and Observations

Star	R.A.[a] (2000)	Decl. (2000)	V	H	K	Exposure (s)	S/N
HD 122563	14 02 31.85	+09 41 09.95	6.19	3.76	3.73	960	>400
HD 140283	15 43 03.10	−10 56 00.60	7.21	5.70	5.59	960	>400

Note.

[a] Positions and magnitudes taken from the SIMBAD database, http://simbad.u-strasbg.fr/simbad/.

(This table is available in machine-readable form.)

An important H-band high-resolution ($R \simeq 22{,}500$) survey of $>10^5$ stars in the APOGEE (Majewski et al. 2010)[10] experiment is currently underway, with a southern hemisphere extension planned for the near future. The new high-resolution H and K band Immersion Grating Infrared Spectrograph (hereafter IGRINS; Yuk et al. 2010)[11] was commissioned in 2014 May at the McDonald Observatory for use with the 2.7 m Smith Telescope. This instrument has been employed for many studies, but early use has concentrated on young stars, the interstellar medium, and various types of emission nebulae.

Very metal-poor stars have not been prime targets for IR spectroscopy due to their extreme line weakness. But as part of the commissioning effort for IGRINS, we obtained spectra for two well-studied halo stars with [Fe/H] < −2: the red giant HD 122563 and the subgiant HD 140283. In this paper, we consider what abundance information can be extracted from these high-resolution, very high signal-to-noise ratio (S/N) spectra that encompass the complete photometric H and K bands. In Section 2 we describe IGRINS, the observations of our stars, and basic data reductions. Section 3 brings in previously collected high-resolution optical data for HD 122563 and HD 140283 in order to derive new model atmospheric parameters for these stars. The derivation of abundances from the IGRINS spectra are contained in Section 4, and discussion of these results appears in Section 5.

2. OBSERVATIONS AND REDUCTIONS

We obtained high-resolution, high S/N (S/N > 400, per resolution element) spectra of HD 122563 and HD 140283 with IGRINS during an instrument commissioning run on the night of 2014 May 23. In Table 1, we give basic data and observational parameters for these stars.

Extended descriptions of IGRINS are given in Yuk et al. (2010) and Park et al. (2014); here we highlight some of its characteristics. Usage of a silicon immersion echelle grating enables this spectrograph to achieve high resolving power, $R \equiv \lambda/\Delta\lambda \simeq 45{,}000$ in both H and K wavelength regions. IGRINS employs two $2K \times 2K$ pixel Teledyne Scientific and Imaging H2RG detectors and it has continuous coverage of both H and K bands $1.48-2.48$ μm, $14800-24800$ Å) together in a single exposure, which allows observers to obtain all the data simultaneously. There is only a small gap between H and K bands of about 100 Å. For point sources such as stars, standard IR observational techniques are employed during data acquisition. That is, four individual exposures of targets and telluric standard stars are taken with an ABBA sequence. A and B nod positions are placed along the 1×15 arcsec slit with a

separation of 7 arcsec. The application of this technique allows one to properly subtract the sky and telescope backgrounds, yielding a clean signal of the targets. Flat field, ThAr lamp and sky exposures are also collected during each night as needed.

For point source observations IGRINS achieves S/N ∼ 100 per resolution element in a one hour exposure on a $K = 10.5$ mag target. Our stars are much brighter (Table 1), and with a total exposure of 960 s we achieved S/N > 400 from photon statistics alone throughout the H and K bands.

To transform the raw data frames into final echelle multi-order (23 in the H-band, 21 in the K-band) spectra we processed the data with the IGRINS reduction pipeline package PLP2 (Lee 2015).[12,13] This suite of tasks in PLP2 automatically performs a variety of reduction procedures: flat fielding, background removal, order extraction, distortion correction, and wavelength calibration. Sky (OH) emission lines were cancelled by subtracting the AB pairs. Once the sky contributions were removed, Th–Ar lamp exposures were used for the initial wavelength calibration. Then the calibration was refined by fitting the OH emission lines in the OH lines appearing in the original "uncancelled" stellar spectra.

Telluric water vapor is the main contaminant in both H and K bands, and CO_2 becomes more effective especially in the latter. Precise removal of the telluric features can be a challenge and needs special attention. Therefore we also observed telluric standards (fast-rotating hot stars, from mid-B to late A-type) at air masses that were very close to those of our target stars. We used the IRAF[14] task *telluric* to divide out the telluric features. This task was performed interactively for each echelle order in the H- and K-band spectra.

The wavelength-calibrated, continuum-normalized, telluric-line-excised echelle spectra were then merged into a single continuous spectrum with the IRAF task *scombine*. The final H- and K-band spectra ready for analysis are shown in Figures 1 and 2. We adopt wavelength units of Ångstroms in these and subsequent figures because we are combining results from optical and IR spectra. These figures are restricted in wavelength to those parts of the H and K bands for which good telluric line removal was achieved; the heavily sky-contaminated (and useless for analysis) band edges are not shown. To demonstrate the very weak-lined nature of HD 122563 and HD 140283 we also plot the reduced IGRINS spectrum of the red horizontal-branch star HIP 54048. This is a solar-metallicity Galactic thin disk red horizontal-branch star with atmospheric parameters

---

[10] Apache Point Observatory Galactic Evolution Experiment; https://www.sdss3.org/surveys/apogee.php.

[11] http://www.as.utexas.edu/astronomy/research/people/jaffe/igrins.html

[12] The pipeline package PLP2 has been developed by the pipeline team led by Jae-Joon Lee at Korea Astronomy and Space Science Institute and by Soojong Pak at Kyung Hee University.

[13] Currently available at: https://github.com/igrins/plp/tree/v2.0.

[14] IRAF is distributed by the National Optical Astronomy Observatory, which is operated by the Association of Universities for Research in Astronomy (AURA) under cooperative agreement with the National Science Foundation.
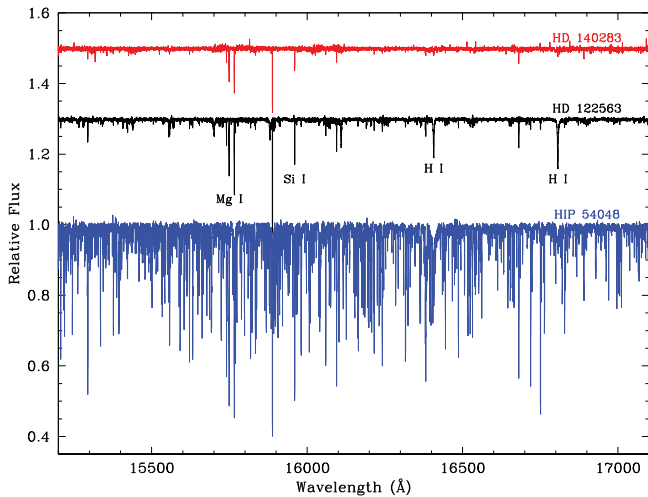
Figure 1. IGRINS H-band spectra of the very metal-poor subgiant HD 140283 (red). The very metal-poor giant HD 122563 (black), and the metal-rich red horizontal-branch star HIP 54048 (blue). The relative flux scale is correct for HIP 54048, and for plotting clarity we have shifted the spectra of HD 122563 and HD 140283 vertically with additive constants. We have trimmed the spectra at the low and high wavelength edges to avoid spectrum regions at the H-band edges with severe telluric contamination. A few prominent features are labeled in the plot, but all of the lines more than a few percent deep in the target star spectra are true stellar absorptions.
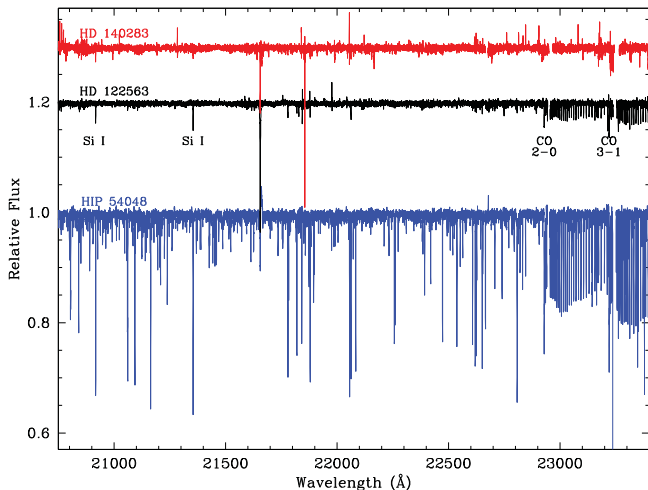

Figure 2. IGRINS K-band spectra of HD 140283 (red). HD 122563 (black), and HIP 54048 (blue). Lines and labels are as in Figure 1.

$(T_{\rm eff}, \log g, [{\rm Fe/H}], \xi_{\rm t}) = (5100\,{\rm K}, 2.65, 0.00, 1.2\,{\rm km\,s^{-1}})$, which were derived by Afşar et al. (2012) from high-resolution optical spectroscopy. The HIP 54048 spectrum is crowded, with many overlapping strong spectral features. In contrast, HD 122563 and especially HD 140283 have few absorption features with central depths as large as 10%. It is clear that both high spectroscopic R and S/N are needed to effectively employ H- and K-band spectroscopy on very metal-poor stars.

3. MODEL ATMOSPHERES AND OPTICAL-REGION ABUNDANCES

Our program stars have been the targets of high-resolution spectroscopy for more than half a century. HD 122563 was the first very metal-poor red giant to have an extensive abundance analysis (Wallerstein et al. 1963), and this honor for very metal-poor subgiants went to HD 140283 (Chamberlain &

Aller 1951). These stars have more than 25 abundance studies each since the year 2000 that are cited in the SAGA Database (Suda et al. 2008).[15] However, in order to make an internally self-consistent comparison of abundances newly derived from IR spectra with those from optical-wavelength spectra, we began by re-determining model parameters for both stars.

The optical spectrum for HD 122563 was obtained with the McDonald Observatory 2.7 m Smith Telescope and echelle spectrograph (Tull et al. 1995) configured to yield $R \simeq 60{,}000$, wavelength coverage $3500\,{\rm \AA} \leqslant \lambda \leqslant 9000\,{\rm \AA}$, and S/N ~ 125 at $\lambda \sim 4500\,{\rm \AA}$, increasing to ~ 250 at $\lambda \sim 6500\,{\rm \AA}$. This spectrum was originally obtained by Westin et al. (2000) to provide a contrasting star to the neutron-capture-rich low metallicity giant HD 115444. We measured equivalent widths (EW) for lines of Fe I, Fe II, Ti I, Ti II, and neutral-species lines of light elements Na, Mg, Al, Si, and Ca, using the spectroscopic manipulation code *SPECTRE* (Fitzpatrick & Sneden 1987). Lines chosen for analysis were those with wavelengths $\lambda > 4500\,{\rm \AA}$ (to avoid significant line blending) that were detectable, isolated, and have well-tested transition probabilities: Ti I, Lawler et al. (2013); Ti II, Wood et al. (2013); Fe I, Den Hartog et al. (2014), Ruffoni et al. (2014), O'Brian et al. (1991); Fe II and the remaining species, the NIST[16] atomic line database (Kramida et al. 2014). The Fe and Ti line parameters and EWs are listed in Table 2 and those of other species are in Table 3.

Since HD 140283 is 1150 K hotter and has a gravity more than two dex higher than HD 122563, it has a much weaker-lined spectrum. Therefore we were able to measure EWs of only about half as many atomic lines for this star. Our main spectrum for this task was originally part of an investigation of the blue metal-poor star CS 29497–030 (Ivans et al. 2005). It was obtained with the Keck I High Resolution Echelle Spectrometer (HIRESb, Vogt et al. 1994). It has $R \simeq 40{,}000$, wavelength coverage $3050\,{\rm \AA} \leqslant \lambda \leqslant 5900\,{\rm \AA}$, and S/N ~ 250 at $\lambda \sim 4500\,{\rm \AA}$, increasing to ~ 300 at $\lambda \sim 5800\,{\rm \AA}$. To measure a few lines redward of $5900\,{\rm \AA}$ we also used a spectrum gathered as part of the large-sample very-metal-poor halo star survey of Roederer et al. (2014). This spectrum, obtained with the Las Campanas Observatory *Magellan* Inamori Kyocera Echelle (MIKE) spectrograph (Bernstein et al. 2003), has $R \simeq 35{,}000$, $5000\,{\rm \AA} \leqslant \lambda \leqslant 8500\,{\rm \AA}$, and S/N ~ 140 at $\lambda \sim 6500\,{\rm \AA}$. The EWs measured for these spectra are listed in Tables 2 and 3.

We derived atmospheric parameters for HD 122563 and HD 140283 by determining line-by-line abundances from the EWs and trial model atmospheres interpolated from the ATLAS model atmosphere α-enhanced grid (Kurucz 2011).[17] The abundance computations were carried out with the version of the line analysis code MOOG (Sneden 1973) that includes scattering in the continuum opacity and source function (Sobeck et al. 2011). Model parameters were adjusted by using standard criteria that line abundances of Fe I show no trend with excitation potential χ and equivalent width EW (for $T_{\rm eff}$ and $\xi_{\rm t}$), that the mean abundances of neutral and ionized species agree for Fe and Ti (for $\log g$), and that the assumed model metallicity are consistent with the derived [Fe/H].

Table 2
Parameters of Fe and Ti Lines

λ_{air} (Å)	Species	χ (eV)	log gf	EW_{122563} (mÅ)	EW_{140283} (mÅ)	[X/Fe][a]	[X/Fe][a]
4449.14	Ti I	1.890	0.47	6.4	⋯	0.14	⋯
4450.89	Ti I	1.880	0.32	3.6	⋯	0.02	⋯
4453.31	Ti I	1.430	−0.03	9.3	⋯	0.26	⋯
4455.32	Ti I	1.440	0.13	8.7	⋯	0.08	⋯
4457.43	Ti I	1.460	0.26	15.5	⋯	0.25	⋯
4512.73	Ti I	0.830	−0.40	14.0	2.0	0.09	0.19
4518.02	Ti I	0.820	−0.25	19.0	3.3	0.08	0.26
4527.30	Ti I	0.810	−0.45	14.4	2.7	0.12	0.35
4533.24	Ti I	0.850	0.54	51.9	15.5	−0.05	0.22
4534.78	Ti I	0.830	0.35	42.5	11.1	−0.03	0.23

Note.
[a] The solar abundances are taken from Asplund et al. (2009); for Fe I and Fe II, the abundances are expressed as [Fe/H].

(This table is available in its entirety in machine-readable form.)

Table 3
Parameters of Other Species Lines

λ_{air} (Å)	Species	χ (eV)	log gf	EW_{122563} (mÅ)	EW_{140283} (mÅ)	[X/Fe][a]	[X/Fe][a]
6300.31	[O I]	0.000	−9.72	syn	⋯	0.76	⋯
6363.78	[O I]	0.020	−0.19	syn	⋯	0.79	⋯
5889.95	Na I	0.000	0.11	182.0	120.0	0.27	0.22
5895.92	Na I	0.000	−0.19	155.0	88.0	0.15	−0.01
8183.26	Na I	2.100	0.24	15.0	⋯	−0.08	⋯
8194.79	Na I	2.100	0.54	30.5	⋯	0.00	⋯
22056.43	Na I	3.191	0.29	syn	⋯	−0.23	⋯
23379.14	Na I	3.753	0.54	syn	⋯	0.02	⋯
4167.17	Mg I	4.350	−0.75	50.8	25.8	0.45	0.35
4571.10	Mg I	0.000	−5.62	82.5	7.0	0.36	0.21

Note.
[a] The solar abundances are taken from Asplund et al. (2009).

(This table is available in its entirety in machine-readable form.)

After model iterations, we obtained atmospheric parameters effective temperature, surface gravity, microturbulent velocity, and model metallicity $(T_{eff}/\log g/\xi_t/[M/H]) = (4500\,K/0.80/2.20\,km\,s^{-1}/−2.90)$ for HD 122563 and $(5650\,K/3.40/1.70\,km\,s^{-1}/−2.70)$ for HD 140283. These parameters are consistent with past analyses of these two stars. Straight averages of all the SAGA entries for each star yield parameters $(4570\,K, 1.1, −2.7)$ for HD 122563 and $(5730\,K, 3.6, −2.5)$ for HD 140283. Our derived metallicities are about 0.2 dex lower than these means of previous studies. A small part ($\sim$0.05 dex) of this metallicity offset is attributable to the use of the scattering-included version of MOOG. The more important reason is that our derived temperatures are lower by about 75 K than the average of entries in the SAGA database. Those previous studies that derive T_{eff} values similar to ours typically also derive [Fe/H] similar to ours.

We then derived abundances of light elements Na, Mg, Al, Si, Ca from all of their neutral-species transitions that have log gf values given in the NIST database and EWs greater than 2.5 mÅ. For the purposes of this paper, we ignored all other elements beyond Ca ($Z = 20$) because they are not detected in our IGRINS spectra. Because there is no single literature source for the transition probabilities of these elements that encompasses the optical and IR spectral domains, we opted to adopt the log gf values from NIST, ignoring for our work the NIST

quality estimates of these values. Derived abundances from individual transitions are given in Table 3, and species means are given in Table 4.

4. THE INFRARED ANALYSIS

Using our high quality IGRINS H- and K-band spectra, we were able to determine abundances of light elements C, O, Na, Mg, Al, Si, S and Ca in HD 122563, and Mg, Al and Si in HD 140283. All of the abundance computations were accomplished with synthetic/observed spectrum matches. As mentioned in Section 3, the much weaker-lined spectrum of HD 140283 yielded only about half as many abundances compared to HD 122563. In this section we discuss the atomic/molecular data choices and describe some details of the abundance analysis.

4.1. Atomic and Molecular Data

To create synthetic spectrum line lists we combined the best atomic and molecular literature data from several sources. We generated the line list by initially adopting atomic and CO molecular lines in selected regions of the H- and K-bands from the Kurucz (2011) database.[18] Then we added CN and OH

---

[18] Available at http://kurucz.harvard.edu/linelists.html.

<div align="center">

Table 4
Mean Abundances

</div>

Species	[X/Fe] 122563	σ 122563	Num 122563	[X/Fe] 140283	σ 140283	Num 140283
CH-vis	−0.28	0.03	CH-band	...	...	...
CO-IR	−0.15	0.06	38	...	...	...
[O I]-vis	0.78	0.02	2	...	...	...
OH-IR	0.92	0.06	51	...	...	...
Na I-vis	0.09	0.16	4	0.11	0.16	2
Na I-IR	−0.11	0.18	2	...	...	...
Mg I-VIS	0.47	0.08	8	0.26	0.06	7
Mg I-IR	0.45	0.03	5	0.27	0.11	6
Al I-vis	−0.70	...	1	−0.99	...	1
Al I-IR	−0.04	0.06	4	−0.29	0.00	2
Si I-vis	0.49	0.20	7	0.51	0.20	3
Si I-IR	0.45	0.05	11	0.33	0.05	9
S I-vis	...	...	...	...	...	...
S I-IR	0.52	0.04	3	...	...	...
Ca I-vis	0.32	0.13	23	0.36	0.09	14
Ca I-IR	0.38	0.18	6	...	...	...
Ti I-vis	0.12	0.09	38	0.27	0.07	13
Ti II-vis	0.29	0.07	39	0.34	0.08	19
Fe I-vis	−2.92[a]	0.12	143	−2.71	0.05	66
Fe II-vis	−2.98[a]	0.10	12	−2.77	0.06	9

Note.
[a] For Fe only the value is [Fe/H].

molecular lines from recent lab publications by Sneden et al. (2014) and Brooke et al. (2016).

Bandheads of the CO ground electronic state first overtone ($\Delta v = 2$) system are prominent in K-band spectra of cool stars (Figure 2), and second overtone lines ($\Delta v = 3$) occur throughout their H-band spectra. We initially adopted CO transition data from the Kurucz database, which were generated from the calculations of Goorvitch (1994). We then tested these line lists by calculating synthetic CO spectra of the solar photosphere with these lines, adopting a solar model atmosphere interpolated in the Castelli & Kurucz (2003) grid with parameters (T_{eff}/log g/ξ_t/[M/H]) = (5780 K/4.44/0.85 km s^{-1}/0.00) and well-determined C and O abundances from optical features (e.g., Asplund et al. 2009 and references therein). These synthetic spectra were compared to the solar photospheric flux spectrum of Wallace & Livingston (2003). The H-band $\Delta v = 3$ "second overtone" lines showed satisfactory synthetic/observed spectrum agreement with the abundances deduced from the optical region. However the K-band $\Delta v = 2$ computed lines were too strong compared to the observed ones, and an increase in C abundance of ~0.2 dex was needed to resolve the discrepancy.

We also synthesized the spectrum of Arcturus (Hinkle & Wallace 2005),[19] adopting an interpolated ATLAS model atmosphere with parameters (4285 K/1.66/1.74 km s^{-1}/−0.52; Ramírez & Allende Prieto 2011) and the C and O abundances of Sneden et al. (2014). Very similar results were obtained: good synthetic/observed agreement for the second overtone bands but the same underprediction of the first overtone bands. Resolution of this discrepancy is beyond the scope of this work, but it has been explored in detail in other investigations (e.g., Ayres et al. 2013 and references therein), with the probable culprit being inadequacies in one-dimensional atmospheric modeling. For the present purposes, we

simply decided to increase the log gf values of the $\Delta v = 2$ first overtone lines by 0.15 dex. We then re-applied these new log gf values to the solar and Arcturus spectra; resulting C abundances yielded good agreement between the optical and H-band abundances.

To find suitable atomic lines we began with the lists of Hinkle et al. (1995) that accompany their infrared Arcturus atlas, and then searched for them in our HD 122563 and HD 140283 spectra. Transition probabilities for the chosen lines were collected from the NIST database, when available. The NIST database does not include log gf recommendations for IR Ca I lines, so we applied reverse solar analysis to determine their log gf values. For this task we again used the Wallace & Livingston (2003) high-resolution infrared solar flux spectrum. Ca I transition probabilities determined in this manner were then tested on the Hinkle & Wallace (2005) spectrum of Arcturus. Good agreement was found with the Arcturus Ca abundance derived by Ramírez & Allende Prieto (2011).

4.2. Abundance Analysis

The near-infrared spectra of cool stars contain many molecular lines, especially OH and CO. Even at low metallicities the possibility exists that atomic lines may be blended. Thereby, we decided to apply the spectrum synthesis technique to all available infrared lines (Table 3) to derive the elemental abundances of C, O, Na, Mg, Al, Si, S and Ca.

Transitions of α-elements Mg, Si, S, and Ca were detected in our IGRINS spectrum of HD 122563, and Mg and Si were represented by lines in both H- and K-bands in both program stars; see Table 3. These IR lines significantly improve the abundances deduced from the optical transitions. Derived mean abundances are presented in Table 4.

In Figure 3, we display 10 Si I lines in the HD 122563 spectrum. The top panels show the violet 3905 and 4102 Å features, the only strong Si I in very metal-poor stellar spectra.

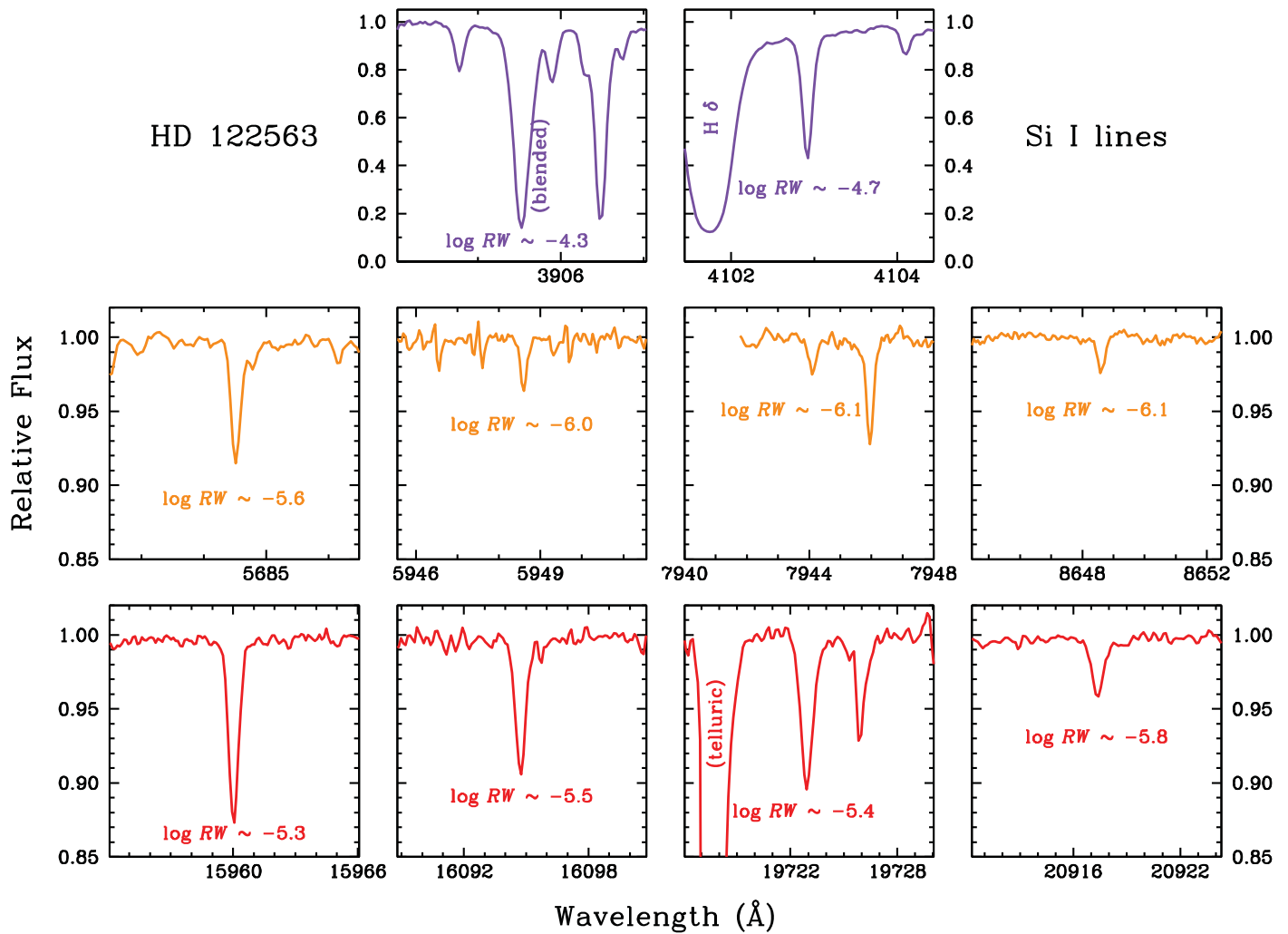[19] Available at ftp://ftp.noao.edu/catalogs/arcturusatlas/.

Figure 3. Small spectral regions surrounding 10 Si I lines in HD 122563. In each panel we have recorded the approximate value of the Si I line reduced width in logarithmic units, log RW ≡ log(EW/λ), which indicates the line strength. Vertical lines are drawn at the line wavelengths. The top panels display in violet the two strong lines usually used for Si abundance studies in very low metallicity stars. The middle panels show in orange four other typical optical-region lines, and the bottom panels show in red four representative H- and K-band lines.

The 4102 Å line's continuum is the wing of Hβ, and the 3905 Å line is partially blended. Moreover, a standard abundance analysis of the 3905 Å line yields T_{eff}-dependent Si abundances (e.g., Sneden & Lawler 2008 and references therein). All other optical-region Si I transitions are very weak in HD 122563, as illustrated in the four middle panels of Figure 3. Only the 5684 Å line has a depth of more than a few percent. These lines are rarely encountered in studies of very metal-poor stars. In contrast, we easily detect more than a dozen Si I lines with reasonably well-determined transition probabilities as judged in the NIST compilation. The optical-region Si detection problems for HD 140283 are even more severe, as only three lines (3905, 4102, and 5684 Å) lines could be measured in our spectra. But our IR abundance is based on nine lines. Additionally, the line-to-line scatters for both stars are significantly smaller in the IR lines than in their optical counterparts. The abundances of Si derived from our IR spectra are clearly more reliable than those from the optical data.

Many of the same comments on Si I could be applied to the Mg I lines in our program stars. Strong IR lines can be easily used for Mg abundances, as we illustrate in the top panel of Figure 4. Here we also show synthetic spectrum matches to all

the features in this wavelength interval. Inspection of these Mg I line profiles suggests that EW analysis could have accomplished the abundance derivation task. But other IR spectral features would require synthetic spectrum calculations, and so we have applied the synthetic spectra to all IR transitions. For Mg I the optical transitions are more competitive with the IR ones in quantity and quality, with the line-to-line abundance scatters being comparable (Table 4). The increase in Mg abundance reliability comes from the merging of results from both optical and IR bands (Figure 5).

Three lines of S I can be detected in HD 122563. However, as seen in the bottom two panels of Figure 4, they are extremely weak, with central depths of $\lesssim$1%. Unsurprisingly, these lines proved to be too weak for detection in HD 140283. From our synthetic spectrum calculations we derived an abundance for HD 122563 of $\langle \log \epsilon(S) \rangle = 4.72$) from the 15470, 15478 and 22707 Å S I lines, or [S/H] = −2.40, [S/Fe] = +0.52. HD 122563 was included in the S abundance survey of Spite et al. (2011), who studied two stronger S I lines at 9228 and 9237 Å. They derived [S/Fe] = +0.42 with a 3D +NLTE calculation, and a purely LTE abundance roughly
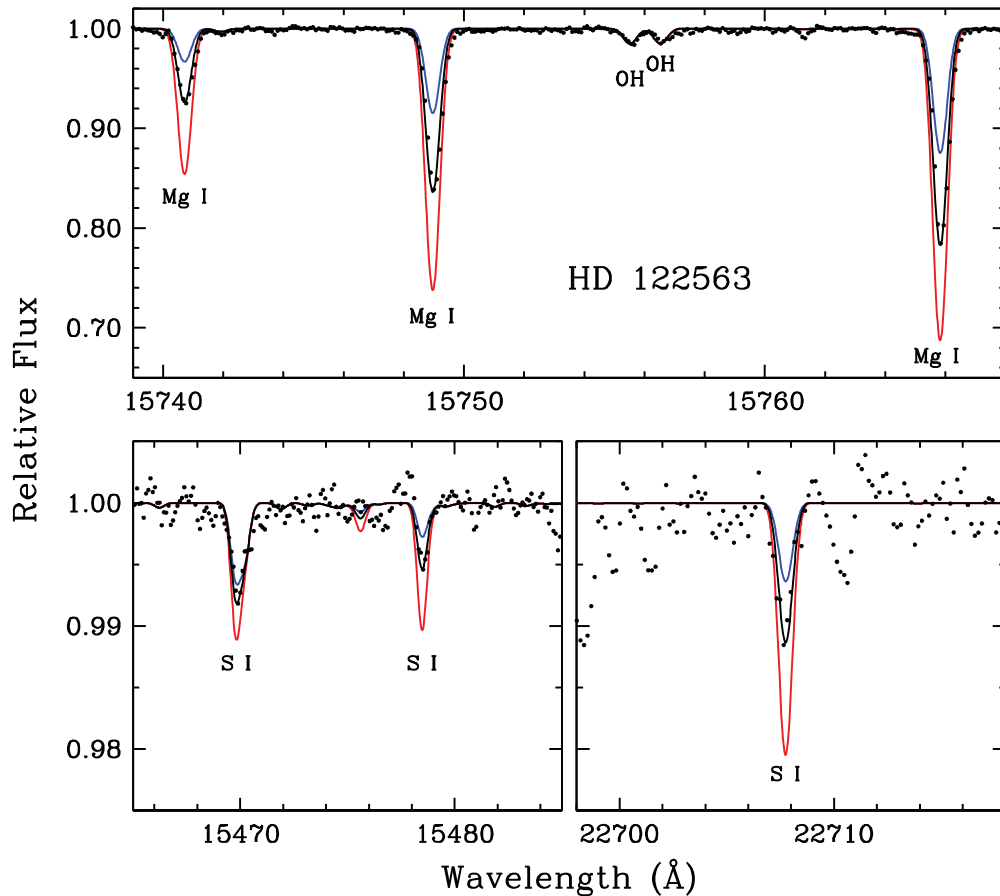
Figure 4. Observed and synthetic spectra of Mg (top panel) and S I (bottom panels) lines in the H- and K-bands. In each panel the small filled circles show the observed spectrum, and the black line represents the synthetic spectrum with an abundance that best matches the transitions in that panel. In the top panel the red and blue lines correspond to synthetic spectrum abundance choices that are offset from the best fit by ±0.4 dex. In the bottom panels the red and blue lines are for synthetic spectrum abundances offset by ±0.3 dex.

0.3 dex larger. To our knowledge, NLTE computations have not been done for our lines, but since they have high excitation energies, $\chi \gtrsim 8.0$ eV, we suspect that they might not be negligible. Future investigation of this issue will be worthwhile. However, our S/Fe overabundance for HD 122563 is in good agreement with previous studies of low metallicity stars (Nissen et al. 2004, Spite et al. 2011, Caffau et al. 2014). Nearly all published S abundances have been based on the S I lines shortward of 10000 Å. IGRINS now gives us a new set of lines to conduct large-sample surveys of this element.

Six IR Ca I lines were detectable in our HD 122563 (Table 3) spectrum, but all were too weak to be seen in HD 140283. There is good agreement between the HD 122563 Ca abundances derived from the optical and infrared regions (Table 4), and indicate [Ca/Fe] $\simeq 0.35$, consistent with Ca overabundances observed in most low-metallicity stars.

Our IGRINS spectra contain a few transitions of odd-Z species Na I and Al I. Two weak Na lines could be detected for HD 122563 in the K-band (Table 3). The mean abundance, $\langle$[Na/Fe]$\rangle = -0.11$ is 0.2 dex smaller than the mean from the three optical-wavelength lines (Table 4), but the line-to-line abundance scatters are large, $\sigma \geqslant 0.16$. The overall mean Na abundance is compatible with previously reported values for very metal-poor stars (e.g., Cayrel et al. 2004; Yong et al. 2013, and references therein).

In our optical-wavelength spectra only the Al I resonance doublet at 3944 and 3961 Å can be detected, and the 3944 Å line has long been known (Arpigny & Magain 1983) to be severally contaminated by CH. The 3961 Å line indicates a large Al deficiency in our stars, [Al/Fe] $\lesssim -0.9$ in our LTE analysis. Although we could not detect other well-studied optical-region higher-excitation Al I doublets (e.g., 6696/ 6698 Å, 7835/7836 Å, or 8772/8773 Å), abundances reported in the literature on metal-poor stars from these lines computed in LTE analyses are [Al/Fe] ~ 0. This clash between the resonance lines and other Al I lines is well-documented, e.g., François (1986), Ryan et al. (1996), and is a clear example of NLTE effects in resonance line formation in metal-poor stars. Baumüller & Gehren (1997) performed a detailed NLTE analysis of Al in subgiants and main sequence stars over a range of metallicities, showing that NLTE Al abundance corrections are much larger for the resonance lines than that higher-excitation ones. For Cayrel et al. (2004)s survey of very metal-poor giants, which included HD 122563, a uniform NLTE correction of +0.65 was adopted for the 3961 Å line. If we apply that to our LTE value of [Al/Fe] $= -0.70$ (Table 4) we obtain -0.05, in agreement with [Al/Fe] $= -0.04$ from the four IR lines. Assuming that a similar correction applies to the LTE abundance derived from the 3961 Å line in HD 140283 yields similar agreement with those derived from the two IR lines, [Al/Fe] $\simeq -0.3$.

HD 122563
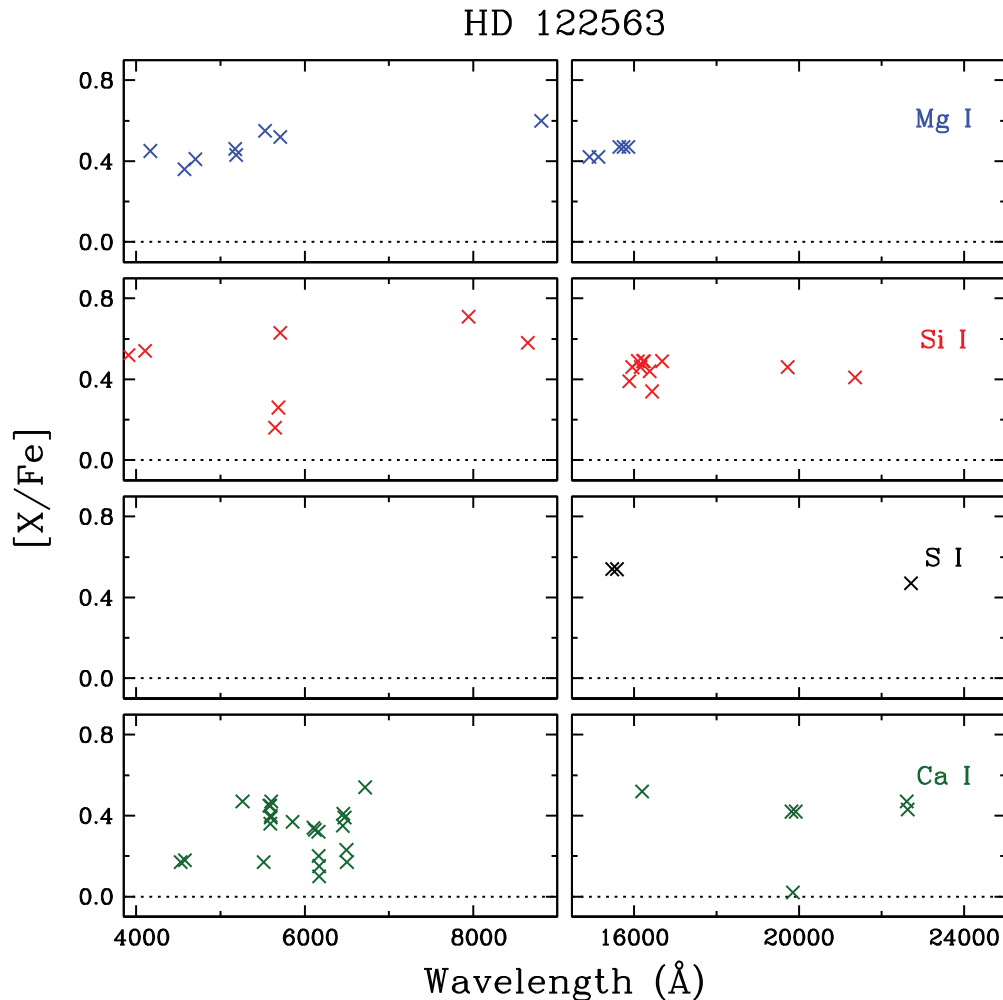

Figure 5. Relative abundance ratios [X/Fe] of α elements (Mg, Si, S, and Ca from top to bottom panels) in HD 122563. The left-hand panels are for abundances derived from the optical-region spectrum, and the right-hand panels are for IGRINS-based abundances.

Many individual OH molecular transitions can be found in the IGRINS H-band spectrum of HD 122563, and many CO transitions in its K-band spectrum. The persistence of detectable OH in this very low metallicity giant is due to the combined effects of: (a) the well-documented O overabundance (many studies beginning with Lambert et al. 1974, [O/Fe] $= -0.6$); (b) the weak formation of the competing double-metal molecule CO; and (c) the (relative) strengthening of hydride molecules with decreasing metallicity (due to increasing gas pressure). Using the new OH ro-vibrational line lists of Brooke et al. (2016), we derived O abundances from 51 OH lines (Table 3), which yielded a mean abundance [O/Fe] $= +0.92$ ($\sigma = 0.05$; Table 4). This value is somewhat larger than the abundance that we derived from the two optical-spectrum [O I] lines, [O/Fe] $= +0.78$. However, recently Dobrovolskas et al. (2015) have carried out detailed 3D atmospheric modeling of [O I] and OH ro-vibrational features in red giants including HD 122563, finding little change of the forbidden lines compared to 1D analyses but decreases of 0.2 -0.3 dex in derived O abundances from the OH lines. Detailed comparisons with their work are beyond the scope of this work, but a correction of this order of magnitude would bring the derived O abundance into satisfactory agreement with O abundance estimates for HD 122563. Due to the large

temperature sensitivity of molecular features, we were unable to detect either OH or CO in HD 140283.

As described in previous section, we raised the log gf values of K-band CO lines by 0.15 dex in order to have a self-consistent C abundance from both optical (CH) and infrared (CO) transitions. For CO we adopted the O abundance derived from OH, and varied the C abundance in the syntheses. The C abundance could only be determined for HD 122563 using the $\Delta v = 2$ first overtone lines that appear in the K-band. Second overtone line ($\Delta v = 3$) strengths are too weak to be detected in either stars. We derive a larger abundance from CO by 0.13 dex than from CH. However, CO molecular line strengths have larger temperature sensitivity than do the CH or OH lines, because of the large dissociation difference between the two molecules. The molecular Saha equation includes the dissociation energy in the exponential term $\exp(-D_0/kT)$, or in logarithmic units $-D_0\theta$, where $\theta \equiv 5040/T$. The dissociation energies of these molecules of $D_0(CH) = 3.47$ eV, $D_0(OH) = 4.39$ eV, and $D_0(CO) = 11.09$ eV. For HD 122563 a 100 K T_{eff} change from our assumed T_{eff} would alter the derived O abundance from OH by $\simeq$0.11 dex, alter the C abundance from CH by $\simeq$0.09 dex, but will change the derived C abundance from CO by $\simeq$0.28 dex. A small temperature decrease would bring agreement to the CH- and CO-based C abundances. We therefore suggest that to first

approximation both C abundance indictors are in accord. The same molecular Saha argument will easily show why neither OH or CO infrared bands can be detected in HD 140283, whose $T_{\rm eff}$ is 1150 K hotter.

Finally, we have considered the effects on our derived abundances for HD 122563 that would occur if we adopt the model atmospheric parameters derived by Creevey et al. (2012). Those authors derived the angular diameter for HD 122563 from interferometry, and combined that value with photometric and astrometric data to recommend $T_{\rm eff} = 4598$ K, $\log g = 1.60$, and [Fe/H] $= -2.6$. We re-derived abundances with this model, finding a metallicity similar to theirs and abundance ratios [X/Fe] from atomic lines very little changed from our values. The abundances of C estimated from CH and O from OH molecular features were also very little affected by the model change. The higher $T_{\rm eff}$ of the Creevey et al. (2012) model yields weaker CH and OH lines, while the much larger $\log g$ strengthens these lines; the two effects counter each other almost completely. However, O abundances derived from [O I] lines becomes about a factor of two larger than that derived from OH due to the large gravity sensitivity of [O I]. Additionally, CO lines have very large sensitivity to $T_{\rm eff}$ (see the discussion in 4.2), so adoption of the Creevey et al. (2012) model would yield C abundances again about a factor of two larger than we have derived. We note that with our lower cooler, lower gravity model we get roughly the same C and O abundances from all relevant species, but that is only a consistency argument. Further study of HD 122563 models would be welcome.

5. DISCUSSION AND CONCLUSIONS

We used the new McDonald Observatory IGRINS high-resolution spectrograph to investigate the IR spectra of two very metal-poor halo stars, HD 122563 and HD 140283. Very few neutral-species transitions are detectable, mainly α-elements. Although our targets are well studied in the optical region, we decided to re-derive the model atmosphere parameters in order to have internal self-consistency in optical and IR analyses. We used these model atmospheres to determine the abundances of species from lines that have been identified in the IR spectrum of Arcturus. We were able to determine the abundances of C, O, Na, Mg, Al, Si, S and Ca in HD 122563, while only Mg, Al and Si were detectable in HD 140283 due to its higher surface temperature compared to HD 122563.

The abundances of α-elements determined from the IR spectra were generally in good agreement with their optical counterparts (Figure 5). Many of the Mg and Si absorption lines in the IGRINS spectra of both HD 122563 and HD 140283 are strong (Figure 3), and yielded more reliable abundances than that of obtained from the visible spectra.

Sulfur is one of the α-elements that is produced via oxygen burning during the core-collapse of massive stars. It plays an important role in deciphering the Galactic alpha-element chemical evolution. The expected flat behavior observed in the [α/Fe]–[Fe/H] plots is still a matter of debate, especially due to limited blend-free optical lines used to investigate this relation. On the other hand, we could detect three extremely weak S I lines in the HD 122563 H- and K-band spectra: 15470, 15478 and 22707 Å. The mean abundance derived from these lines indicates that sulfur is enhanced about 0.5 dex as expected for an α-element in very-metal-poor stars (e.g.,

Kacharov et al. 2015). To our knowledge, these H- and K-band S I lines have never been studied for our targets. In fact, the 22707 Å sulfur line has been used for the first time here to determine the sulfur abundance of such a very-metal-poor star. With IGRINS now, we have gained more useful sulfur lines to investigate its complex behavior throughout the Galaxy.

We were also able to detect two odd-Z elements, Na and Al. Both elements were only available in the HD 122563 spectrum. The abundance of Na could be determined, with a significant line-to-line scatter, for HD 122563 from two Na I lines identified in the K-band (Table 3). However, Na did not reveal itself in the spectrum of HD 140283. The abundances of aluminum determined for both stars yielded a solar value, which is compatible with the NLTE-corrected abundances obtained from the resonance lines at 3944 and 3962 Å (e.g., Andrievsky et al. 2008) for very metal-poor stars. This promising result indicates that IR Al I lines might be used for NLTE-free abundance determination, especially for very metal-poor stars that suffer from severely contaminated aluminum lines in the blue part of the optical region. More definitive conclusions await further investigation of the IR Al I lines in a large sample of very metal-poor stars.

Looking to future high-resolution IR spectroscopic studies of very metal-poor stars, what could be the low metallicity limit for useful information? Here we consider only red-giant stars like HD 122563 due to their stronger-lined spectra than subgiants or main-sequence stars at similar metallicities. One of the stronger lines in our atomic list is Si I at 15888 Å. Its central depth is over 30% in the HD 122563 spectrum. When we assume a S/N $\simeq 100$ and adopt an approximate value of [Si/Fe] $\simeq +0.50$ for very metal-poor stars with atmospheric parameters similar to those HD 122563, the 15888 Å line appears to be still detectable with a central depth of about 8% for an extremely metal-poor star ([Fe/H] $\simeq -4$). This simple experiment shows us the capacity of IGRINS to detect at least a few species in red giants even more metal-poor than HD 122563.

OH and CO lines are very weak in HD 122563, with $\sim$1 -4% central depths. However, there are many that can be detected in its spectrum. We used 51 OH and 38 CO lines to form our abundance means for O and C. Therefore, as a detection experiment we selected one K-band echelle order and first shifted 16 CO lines that appear in it from their rest positions to a common scale referenced to their line centers. We overplot these shifted absorption features in panel (a) of Figure 6. We then co-added them to produce an "average" CO line; this is displayed in the panel (b) of Figure 6. A similar line averaging exercise was done for UV CO lines by Frebel et al. (2007). While the original spectrum has high S/N, S/N $\simeq 450$ in this wavelength region, the co-added spectrum has S/N $\simeq$ 1000. The average line, although just 3% deep, can be easily analyzed.

We have computed synthetic spectra with parameters characteristic of the 16 CO lines under consideration (excitation energy $\chi = 0.11$, transition probability -5.72), and plot the results in panel (c) of Figure 6. For this test the absolute abundance of CO was not important. We matched the observed average line as closely as possible, and then repeated the synthesis several times with abundances shifted in abundance steps of 0.3 dex. Visual inspection of the observed/synthetic spectrum matches, and in the observed *minus* computed spectrum differences shown in panel (d) of the figure, suggest
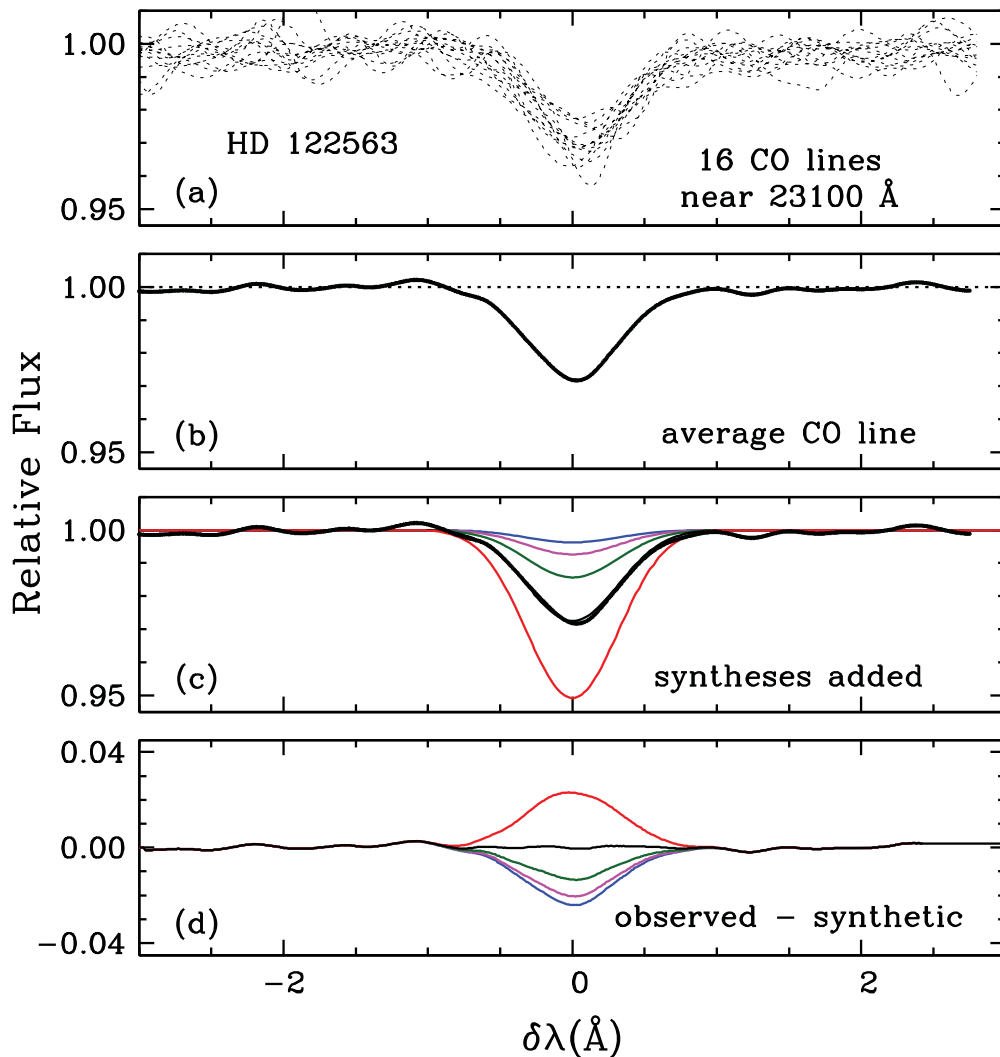
Figure 6. Observed and synthetic spectra of CO first-overtone lines in HD 122563. Panel (a): 16 individual lines near 23100 Å are shown, shifted together in wavelength space by subtraction of their central wavelengths. Panel (b): the co-addition of these 16 lines is shown. Panel (c): the co-added observed spectrum is again plotted, along with five synthetic spectra generated with the model atmosphere adopted for HD 122563 and a single CO line with a mean excitation potential and transition probability of the co-added observed lines. The synthesis drawn with a black line, nearly indistinguishable from the observed line, has C and O abundances chosen to best match the observation. The other synthetic spectrum lines are: red for a C abundance 0.3 dex larger than the best fit, green for 0.3 smaller, magenta for 0.6 smaller, and blue for 0.9 smaller. Panel (d): the difference be observed and computed spectra.

that the double-metal molecule CO can be detected in red-giant stars with metallicities at least 0.3 dex lower than HD 122563.

Detections of atomic transitions will not be easy at lower metallicities than HD 122563. As mentioned above, the strongest line in our H- and K-band spectra of this star is Si I 15888 Å. Our numerical experiments suggested that this line might be detectable in stars with metallicities as low as [Fe/H] ~ -4. The atmospheric parameters of HD 122563 place it close to the very metal-poor red-giant tip. The most luminous red giant members of the lowest metallicity globular clusters have temperatures and gravities as small as $T_{\rm eff} \sim 4250$ K and $\log g \sim 0.0$. Such stars would have stronger-lined spectra than HD 122563 at [Fe/H] ~ -3, thus would be attractive IGRINS targets. However, stars bright enough for IGRINS observations are not plentiful. It may be as interesting to explore the spectra of somewhat higher metallicity stars; our search for detectable transitions in HD 122563 and HD 140283 suggests that other species such as K I may exhibit useful lines for stars with [Fe/H] ~ -2.

In this paper, we have shown that many light elements have neutral transitions that can be usefully applied to abundance analyses of very metal-poor stars. These spectral features are consistent with and in several cases appear to be more reliable abundance indicators than transitions in the optical spectral range. Future IGRINS observations of stars spanning the metal-poor metallicity domain should be undertaken.

REFERENCES

Afşar, M., Sneden, C., & For, B.-Q. 2012, AJ, 144, 20
Andrievsky, S. M., Spite, M., Korotin, S. A., et al. 2008, A&A, 481, 481
Arpigny, C., & Magain, P. 1983, A&A, 127, L7
Asplund, M., Grevesse, N., Sauval, A. J., & Scott, P. 2009, ARA&A, 47, 481
Ayres, T. R., Lyons, J. R., Ludwig, H.-G., Caffau, E., & Wedemeyer-Böhm, S. 2013, MSAIS, 24, 85
Baumüller, D., & Gehren, T. 1997, A&A, 325, 1088
Bernstein, R., Shectman, S. A., Gunnels, S. M., Mochnacki, S., & Athey, A. E. 2003, Proc. SPIE, 4841, 1694
Brooke, J. S. A., Bernath, P. F., Western, C. A., et al. 2016, JQSRT, 168, 142
Caffau, E., Monaco, L., Spite, M., et al. 2014, A&A, 568, A29
Castelli, F., & Kurucz, R. L. 2003, in IAU Symp. 210, Modelling of Stellar Atmospheres, ed. N. Piskunov, W. W. Weiss, & D. F. Gray (San Francisco, CA: ASP), A20
Cayrel, R., Depagne, E., Spite, M., et al. 2004, A&A, 416, 1117
Chamberlain, J. W., & Aller, L. H. 1951, ApJ, 114, 52
Creevey, O. L., Thévenin, F., Boyajian, T. S., et al. 2012, A&A, 545, A17
Den Hartog, E. A., Ruffoni, M. P., Lawler, J. E., et al. 2014, ApJS, 215, 23
Dobrovolskas, V., Kučinskas, A., Bonifacio, P., et al. 2015, A&A, 576, A128
Elias, J. H., Joyce, R. R., Liang, M., et al. 2006, Proc. SPIE, 6269, 62694C
Fitzpatrick, M. J., & Sneden, C. 1987, BAAS, 19, 1129
François, P. 1986, A&A, 160, 264
Frebel, A., Norris, J. E., Aoki, W., et al. 2007, ApJ, 658, 534
Goorvitch, D. 1994, ApJS, 95, 535
Hinkle, K., & Wallace, L. 2005, in ASP Conf. Ser. 336, Cosmic Abundances as Records of Stellar Evolution and Nucleosynthesis, ed. T. G. Barnes, III, & F. N. Bash (San Francisco, CA: ASP), 321
Hinkle, K., Wallace, L., & Livingston, W. C. 1995, Infrared Atlas of the Arcturus Spectrum, 0.9–5.3 microns (San Francisco, CA: ASP)
Ivans, I. I., Sneden, C., Gallino, R., Cowan, J. J., & Preston, G. W. 2005, ApJL, 627, L145
Kacharov, N., Koch, A., Caffau, E., & Sbordone, L. 2015, A&A, 577, A18
Kaeufl, H.-U., Ballester, P., Biereichel, P., et al. 2004, Proc. SPIE, 5492, 1218
Keller, S. C., Bessell, M. S., Frebel, A., et al. 2014, Natur, 506, 463
Kramida, A., Ralchanko, Y., Reader, J. & NIST ASD Team 2014, NIST Atomic Spectra Database (version 5.2) (Gaithersburg, MD: NIST)
Kurucz, R. L. 2011, CaJPh, 89, 417
Lambert, D. L., Sneden, C., & Ries, L. M. 1974, ApJ, 188, 97
Lawler, J. E., Guzman, A., Wood, M. P., Sneden, C., & Cowan, J. J. 2013, ApJS, 205, 11
Lee, J.-J. 2015, plp: Version 2.0, v.2.0.0, Zenodo
Majewski, S. R., Wilson, J. C., Hearty, F., Schiavon, R. R., & Skrutskie, M. F. 2010, in IAU Symp. 265, Chemical Abundances in the Universe: Connecting First Stars to Planets, ed. K. Cunha, M. Spite, & B. Barbuy (Cambridge: Cambridge Univ. Press), 480
Nissen, P. E., Chen, Y. Q., Asplund, M., & Pettini, M. 2004, A&A, 415, 993
O'Brian, T. R., Wickliffe, M. E., Lawler, J. E., Whaling, W., & Brault, J. W. 1991, JOSAB, 8, 1185
Park, C., Jaffe, D. T., Yuk, I.-S., et al. 2014, Proc. SPIE, 9147, 1
Ramírez, I., & Allende Prieto, C. 2011, ApJ, 743, 135
Roederer, I. U., Preston, G. W., Thompson, I. B., et al. 2014, AJ, 147, 136
Ruffoni, M. P., Den Hartog, E. A., Lawler, J. E., et al. 2014, MNRAS, 441, 3127
Ryan, S. G., Norris, J. E., & Beers, T. C. 1996, ApJ, 471, 254
Sneden, C. 1973, ApJ, 184, 839
Sneden, C., & Lawler, J. E. 2008, in AIP Conf. Ser. 990, First Stars III, ed. B. W. O'Shea, & A. Heger (Melville, NY: AIP), 90
Sneden, C., Lucatello, S., Ram, R. S., Brooke, J. S. A., & Bernath, P. 2014, ApJS, 214, 26
Sobeck, J. S., Kraft, R. P., Sneden, C., et al. 2011, AJ, 141, 175
Spite, M., Caffau, E., Andrievsky, S. M., et al. 2011, A&A, 528, A9
Suda, T., Katsuta, Y., Yamada, S., et al. 2008, PASJ, 60, 1159
Tull, R. G., MacQueen, P. J., Sneden, C., & Lambert, D. L. 1995, PASP, 107, 251
Vogt, S. S., Allen, S. L., Bigelow, B. C., et al. 1994, Proc. SPIE, 2198, 362
Wallace, L., & Livingston, W. 2003, An Atlas of the Solar Spectrum in the Infrared from 1850 to 9000 cm^{-1} (1.1 to 5.4 micrometer), NSO Tech. Rep. (Tucson: National Optical Astronomy Observatory)
Wallerstein, G., Greenstein, J. L., Parker, R., Helfer, H. L., & Aller, L. H. 1963, ApJ, 137, 280
Wallerstein, G., & Helfer, H. L. 1959, ApJ, 129, 720
Westin, J., Sneden, C., Gustafsson, B., & Cowan, J. J. 2000, ApJ, 530, 783
Wood, M. P., Lawler, J. E., Sneden, C., & Cowan, J. J. 2013, ApJS, 208, 27
Yong, D., Norris, J. E., Bessell, M. S., et al. 2013, ApJ, 762, 26
Yuk, I.-S., Jaffe, D. T., Barnes, S., et al. 2010, Proc. SPIE, 7735, 77351M